

Applying Photovoltaic Principles to the Design and Development of an Automated Solar Tracker

Aaron Lee

I. Abstract

Solar tracking systems dynamically adjust photovoltaic panel orientation to maintain optimal sun alignment, potentially enhancing energy harvest compared to fixed installations. This study investigates the design, construction, and performance validation of an automated single-axis solar tracker incorporating light-dependent resistor (LDR) sensors, servo motor actuation, and Arduino-based control. We quantified photovoltaic cell response with three key parameters: angle of incidence, spectral wavelength, and tracking versus static operation. The angle of incidence of incoming light was found to greatly affect the power output of the solar cell, which steadily decreased as angle increased; an orthogonal 0° had the highest output. We characterized the output of the solar cell on the spectral wavelength incident on the setup (630nm, 530nm, and 470nm wavelengths), and found discrepancies in the output power favoring longer wavelengths. A laboratory conducted experiment demonstrated nearly eight-fold power improvement (7.9 mW tracked versus 1.0 mW static). The field experiment that is conducted under California sun conditions over a full day (7:30 AM to 6:00 PM) revealed 53.92% increase to average power output (26.32 mW tracked versus 17.10 mW for static panel matched to altitude angle 36.95°). The tracking system maintained superior performance throughout the day graph other than at solar noon, where the power values converged to around the same magnitude as the sunlight reached the point where it was directly incident upon the static solar cell. Temperature control throughout experiments eliminated thermal effects as confounding variables. These findings establish that automated solar tracking provides significant energy harvest enhancement.

II. Introduction

Solar energy is a cornerstone of renewable energy production globally, utilizing the photovoltaic effect to produce electricity from photons striking the surface of a photovoltaic (PV) cell. The efficiency of energy conversion in photovoltaic cells depends on multiple factors, including the angle of light incidence [1], light wavelength [2], and ambient temperature [3]. As the global demand for clean energy increases, optimizing these parameters has become significant for both residential and commercial solar power generation. A proven approach for maximizing the output of a PV cell is through solar tracking, where the angle of a solar cell is changed dynamically to keep the angle of incidence of incoming light to a minimum. This strategy allows the PV cell to intercept the maximum possible amount of light, significantly enhancing energy yield as compared to fixed panels (up to 54%) [4]. Solar trackers are proven to be particularly



valuable in large-scale solar farms, where even modest increases in energy yield result in reduced levelized cost of energy and higher overall project efficiency [5].

This study investigates the practical application of photovoltaic principles in the design and development of a custom-built automated solar tracker. The goals are to quantify the relationship between incident light angle, wavelength, and PV cell output, and to compare the effectiveness of static versus dynamically tracked configurations in both an artificial scenario, and a field test under the California sun. In this study, we aimed to define optimal parameters for maximizing solar energy harvest in realistic scenarios through leveraging a combination of mechanical actuation, sensor feedback, and controlled experimental conditions.

III. Literature Review

Research on automated solar tracking systems has established that dynamic positioning mechanisms can significantly enhance photovoltaic energy output over static installations. Bhuyain et al. designed and constructed a single-axis solar tracking prototype utilizing Light Dependent Resistors (LDRs) for sunlight detection and an ATMega328P microcontroller for servo motor actuation, achieving increased power output through automated panel positioning where maximum light reception occurs [6]. Similarly, Muhsin and Yousif deployed five LDR sensors with Arduino UNO control to rotate solar panels toward maximum light intensity, with field testing revealing tracker-equipped panels generated higher voltage, current, and overall efficiency compared to static panels across multiple time intervals [7]. Shalwala analyzed energy roof-mounted yield increases from prototype solar tracking panels microprocessor-controlled monitoring device with sensors detecting sun position and electric servo motors for adjustment, demonstrating that solar tracking enhanced energy yield by approximately 35.6% over fixed panels on sloped roofs [8]. An experimental investigation by Algarni et al. comparing fixed-tilt, single-axis, and dual-axis tracking mechanisms under clear-sky conditions in Saudi Arabia revealed that dual-axis tracking systems achieved 28.98% higher net energy output than fixed panels, while single-axis systems achieved 18.73% improvement, despite energy losses of 3.9% and 13.0% respectively from actuating mechanisms [9]. Schallenberger et al. documented in Brazil that a solar tracking plant consistently achieved generation efficiency exceeding 30% compared to a fixed plant, with statistical analysis confirming significant differences between tracking and fixed methods during data collection periods in 2021-2022 [10].

What distinguishes this research is its integration of initial laboratory-controlled spectral and angular testing, thermal isolation using a PID system to separate optical from thermal effects, and a custom constructed, simple, and relatively inexpensive dual-axis tracking system achieving nearly 8-fold improvement in controlled settings and 53.92% enhancement in an



outdoor test. While flawed, the simplicity of the build illustrates the implementability of dual axis tracking systems in solar applications.

IV. Materials and Methods

Materials	Price	Description
Solar Cell	\$15.99	5V 200mA Solar Cell, small and lightweight.
Resistors	<u>\$9.99</u>	Used for LDR circuit and as a load for output measurement
Dig. multimeter	\$41.99	Used to measure voltages
Alligator clips	\$5.99	Temporary or test electrical connections
Solder	<u>\$7.99</u>	Final electrical connections
Circuit board	\$8.79	Used to simplify electrical connections
Electrical Tape	<u>\$7.79</u>	Covering soldered connections to prevent short circuits
Arduino Uno	<u>\$33.85</u>	Used to program components together and allow them to work
Linear Actuator	<u>\$31.99</u>	Used to control the panel to match the altitude angle of the sun.
BTS7960	<u>\$10.99</u>	Used to drive linear actuator movement, making it controllable from Arduino UNO
360° continuous Servo	<u>\$29.99</u>	Used to control the panel to match the azimuth angle of the sun.
LDRs	<u>\$7.39</u>	Used to find light intensity as a parameter for servo and linear actuator motion
Heating Pad	<u>\$11.90</u>	Used to heat solar cell
PID Temperature Controller Kit	\$39.99	Used to keep solar cell temperature constant by controlling the heating pad using K type thermocouple value as a parameter
Aluminum plating	<u>\$15.99</u>	Used as a thermal conductor to allow heat to travel from the heating pad to the solar cell
Foam Insulation	\$20.97	Used as a thermal insulator to prevent heat loss, as well as heat damage to other components.



Materials	Price	Description
20x30x1/4" Baltic Birch Plywood	<u>\$22.50</u>	3 purchased. Used to assemble all parts into a working physical product
Hot glue	<u>\$7.60</u>	Used to connect laser cut pieces and construct the build.

Table 1: Materials list for dual axis solar tracker build. Name of material, price, description, and link for purchase are provided. Total price for the entire build was \$331.69.

Tracker Design and Mechanism

The tracker mechanism incorporated a servo motor and linear actuator, which were controlled by an Arduino Uno running an algorithm that maximized light intensity using inequalities of the LDR outputs. Position feedback was provided by 4 LDRs, each mounted on one side of the solar cell, enabling the system to adjust to the highest light incidence dynamically, moving on both axes with the linear actuator and servo toward the LDR outputting the highest lux. The PID temperature controller along with an SSR and K-type thermocouple regulated cell temperature at a constant temperature to minimize data skewing during power measurements by the effects of thermal drift.

Mounting was accomplished with precision laser-cut wood, aluminum plating for efficient heat conductivity between the PID heated pad and the solar cell, hot glue, and foam insulation to prevent heat from seeping into other parts of the tracker. The linear actuation allowed the tracker to rotate the solar panel through precise increments, matching the simulated movement of the light source. Temperature was maintained constant throughout all experiments using a PID-controlled heating system, eliminating thermal effects as a confounding variable and ensuring that observed performance variations were attributable solely to the manipulated parameters (angle, wavelength, and tracking mode).

Preliminary Experiments: Incidence Angle and Color/Spectrum Effects on Power Output

To measure incident angle effects, the cell was tilted in increments using a tripod to hold the LED array steady. The distance between the solar cell and the LED array was kept constant at 40cm. The corresponding power output was recorded for angle values ranging from 0 to 90 degrees in increments of ten. To measure color/wavelength effects, red (630 nm), green (530 nm), and blue (470 nm) LEDs were used, each placed at varying distances to maintain a constant brightness of 130 Lux. Power is measured through a 560 Ohm resistor.

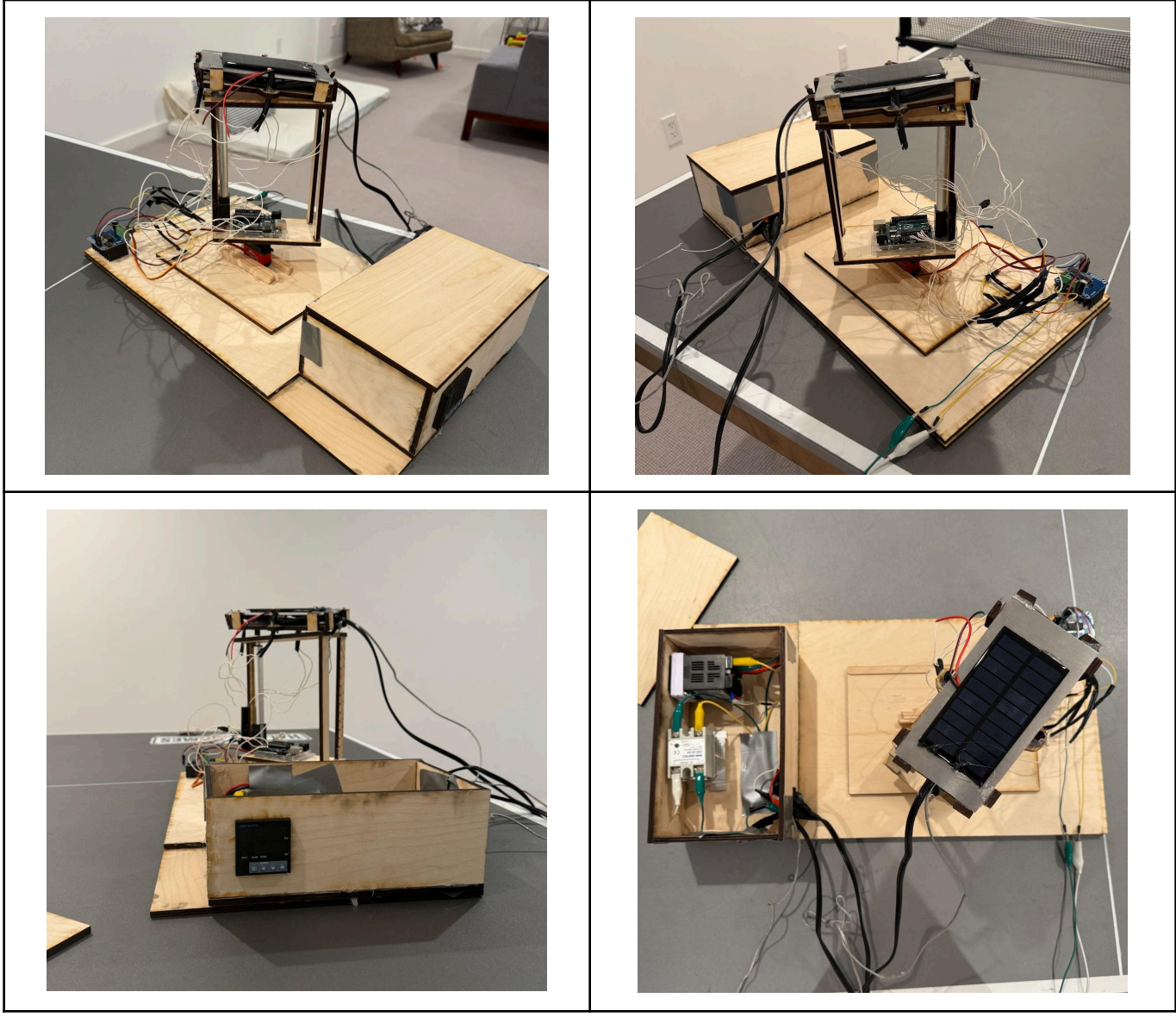


Figure 1: Photos of the dual axis tracker build from multiple angles.

Tracker Test: Simulated scenario Experimental Setup

Two configurations were tested:

- 1. Static Panel: The solar cell was fixed at a 45° incident angle.
- 2. **Tracking Panel**: The solar cell actively followed a moving light source over 180° of simulated sun path, then reversed.

Power output was sampled in 5 second intervals for both static and tracking trials, with voltage measured by a multimeter across a 560 Ohm resistor. For both trials, light starts at a 45° angle with the ground, incident to the panel at 0° (direct light) and 10 cm away. It was then moved



around 180°, then moved back. Power output was calculated by using the equation $P = \frac{V^2}{R}$ derived from fundamental equation P = IV and Ohm's law, V = IR.

Tracker Test: Real World scenario Experimental Setup

The solar tracking apparatus was placed in an area that is brightly lit on a sunny day. Next to it was a static solar cell placed at the angle 36.95°, the altitude angle of the sun at 12:53 P.M (solar noon). Both ran the entire day from 7 A.M to 7 P.M, with voltage measured across a 560 Ohm resistor. Power was calculated using $P = \frac{V^2}{R}$.

V. Results

The experimental results from this study demonstrate clear relationships between photovoltaic cell performance and several key variables, including angle of incidence, light wavelength, and tracking capability. Power output demonstrated a strong dependence on both incident angle and light color, with optimal values recorded at normal incidence and under red illumination. The automated tracking system yielded a substantial increase in average power compared to a fixed panel across the entire tested range.

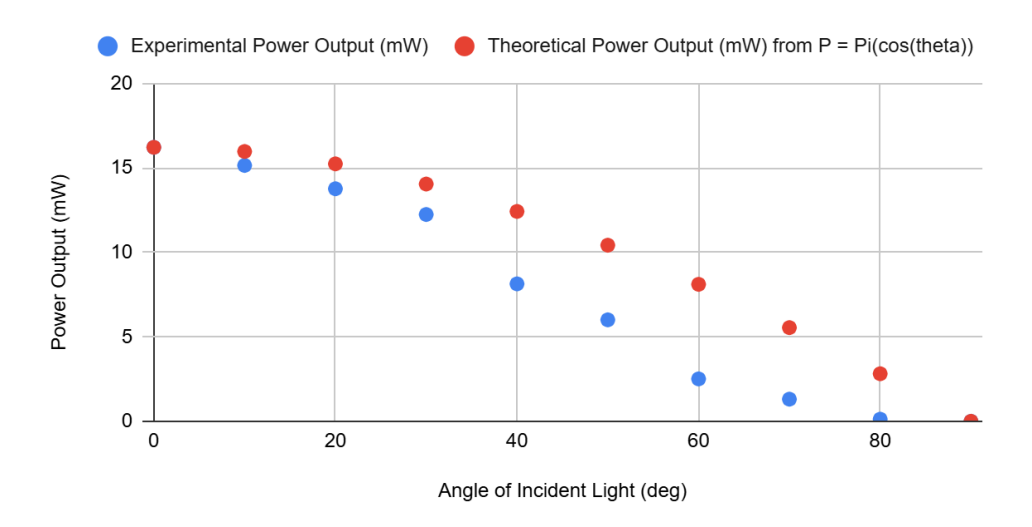


Figure 2. Experimental and Theoretical Power Output (mW) Based on Angle of Incident Light.

Power vs. Angle of Incident Light

The measured power output of the photovoltaic cell decreased as the angle of incidence increased. At 0°, the power output was 16.2 mW, representing the maximum recorded value. The output declined with increments in the panel's tilt, dropping to 12.2 mW at 30°, 1.3 mW at 70°, and reaching 0.1 mW at 80°. The angle of incidence experiments (Figure 2) revealed that



power output decreased systematically as the tilt angle increased from 0° to 90°. However, the measured values remain significantly below the theoretical prediction given by:

$$P_f = P_i cos(\theta)$$

This discrepancy additionally seems to increase with the angle of incident light. A likely cause for this difference is Fresnel reflection at the air-glass interface on the solar cell. When unpolarized light strikes the surface, the reflectance is the average of the s-polarized and p-polarized components [11]:

$$R_{avg}(\theta) = \frac{\left(\left(\left(n_{1}cos\theta - n_{2}cos\theta_{t}\right) / \left(n_{1}cos\theta + n_{2}cos\theta_{t}\right)\right)^{2} + \left(\left(n_{1}cos\theta_{t} - n_{2}cos\theta\right) / \left(n_{1}cos\theta_{t} + n_{2}cos\theta\right)\right)^{2}\right)}{2}$$

where n_1 is the refractive index of air (\approx 1.0), n_2 is the refractive index of the glass cover (\approx 1.5), and θ_t is the transmission angle into the glass given by Snell's law:

$$n_1 \sin\theta = n_2 \sin\theta_t$$

At normal incidence ($\theta = 0^{\circ}$), the reflectance is theoretically only about 4%, but it rises quickly with angle. Around 9% at 60° and nearly 39% at 80°. This means the actual power can be more accurately modeled as:

$$P_f \approx P_i cos\theta * (1 - R_{avg}(\theta))$$

Thus, even though the cosine law captures the geometric projection effect, Fresnel reflection losses at the dielectric interface explain why the experimental curve lies below the theoretical one and why the gap widens as the angle increases.

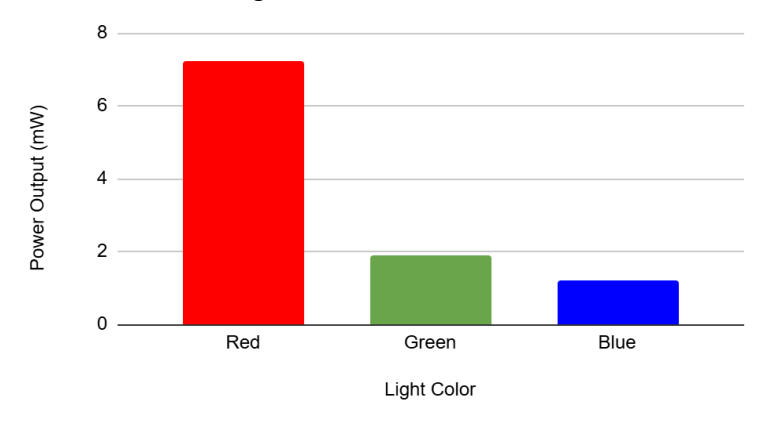


Figure 3. Power Output (mW) vs. Color of Light



Power Output vs. Light Spectrum

The power output of the photovoltaic cell was dependent on the color of incident light. Under red light (630 nm), the cell produced an average power of 7.22 mW. The measured power decreased to 1.90 mW under green light (530 nm) and further to 1.21 mW under blue light (470 nm), all at a constant illumination of 130 lux. These results confirm that the power generated varied substantially with light wavelength. This wavelength dependence can be explained by the spectral response characteristics of silicon-based photovoltaic cells. Silicon solar cells are optimized for longer wavelengths in the red and near-infrared regions because photons at these wavelengths have energies closer to the bandgap, allowing for more efficient electron-hole pair generation with minimal thermalization losses. In contrast, higher-energy blue photons (approximately 2.6 eV) generate excess energy that is dissipated as heat rather than contributing to electrical output. Additionally, blue light has a much shorter absorption depth in silicon (just a few micrometers) compared to red light (which can penetrate hundreds of micrometers), meaning blue photons are primarily absorbed near the surface where recombination rates are typically higher due to surface defects and the presence of the emitter region. The solar spectrum reaching Earth's surface contains a significant proportion of red and near-infrared wavelengths, making silicon's spectral response well-matched to natural sunlight conditions. This inherent optimization for red wavelengths explains why the tested photovoltaic cell demonstrated superior performance under red illumination compared to green or blue light sources.

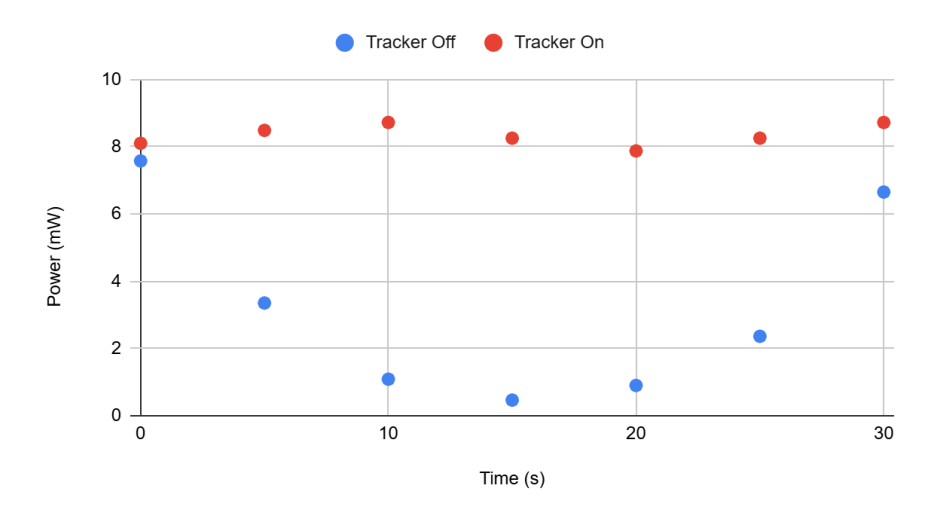


Figure 4: Power Output with Dual Axis Tracker Off vs. Dual Axis Tracker On in a Simulated Environment



Figure 5: Power Output with Dual Axis Tracker On Vs. Dual Axis Tracker Off (Static Panel) Over Time in a Field Experiment

Analysis of the Efficacy of the Solar Tracker

In the static trial, the average power output was about 1.0 mW. When tracking was enabled, the average power over the same period increased to about 7.9 mW, a nearly eightfold increase in power. At each measured time point other than time 0 and 30 (where angle of light was the same), the tracked configuration maintained significantly higher power output than the static configuration.

The tracker was also tested outdoors under actual California sun conditions over a nearly full day from 7:00 AM to 7:00 PM. The tracker-enabled configuration produced an average power output of 26.32 mW while the static panel (tracker off) generated an average of 17.10 mW. This represents a 53.92% improvement in power generation. These real-world results validate the simulated findings from Figure 4, confirming that active solar tracking significantly enhances energy harvest throughout the day under variable sunlight conditions.

The automated tracking system demonstrated substantial performance improvements in both controlled laboratory conditions and real-world deployment. In the simulated sun path experiment (Figure 4), the tracking-enabled configuration achieved an average power output of approximately 7.9 mW compared to 1.0 mW for the static panel positioned at 45°. This nearly eight-fold increase demonstrates the tracker's capability to maintain optimal alignment with the light source throughout its angular trajectory. More significantly, the real-world field test (Figure 5) conducted over a full day from 7:30 AM to 6:00 PM under actual California sun conditions revealed that the tracking system produced an average power output of 26.32 mW compared to 17.10 mW for the static panel (horizontal, 0° tilt), representing a 53.92% improvement in energy generation. Multiplying out to the entire day (12 hours, so 43200 seconds), the total energy



produced by the static panel was 738.61 J, while the dual axis tracked solar panel produced 1149.07 J.

Several discontinuities in power output were observed, most notably at points 10:25, 13:00 and 14:40, where large sudden power drops occurred. These anomalies are likely attributable to transient cloud coverage, which temporarily reduced irradiance levels. Another possibility is human or natural interference with the sunlight incident on the solar cell (Shadows from passing birds, humans, or other animals. Possibly wind blowing a leaf over the cell surface).

Comparison to Known Values

The performance characteristics observed in this study align well with both theoretical predictions and values reported in literature, with some notable considerations. The angular dependence of power output follows the expected cosine relationship [2] modified by Fresnel reflection losses, as demonstrated in the caption of Figure 2. The spectral response favoring red wavelengths is consistent with the known properties of silicon photovoltaic cells, which exhibit maximum efficiency in the 600-900 nm range [3]. The performance of the tracking system also falls within the standard range. Improvement from static to dual-axis tracking systems typically ranges from 39-54% [4]. The solar tracker designed in this experiment had an improvement of 53.92% from the static control test, which is within this range of accepted values.

Solar Tracker Design Flaws

One flaw of the solar tracker is the LDR-based sun-tracking sensors. While effective at directional sensing, they exhibit nonlinear response characteristics and temperature-dependent sensitivity that may affect tracking accuracy, particularly under rapidly changing illumination conditions. The response time of the servo motor and LDR feedback loop introduces a lag between changes in sun position and panel repositioning, potentially resulting in brief periods of suboptimal alignment.

The most major issue with the design of the solar tracker is the fact that the wiring that connects the system to the servo motor, BTS7090, power supply, and PID heater is prone to tangling. The root cause of this issue stems from the fact that the LDR circuit must be connected to the rotating part of the solar cell. A change in the angles of the LDRs away from the positions they are optimized in can severely compromise performance. In order to ensure that little to no force is placed on the LDRs, both the LDR circuit and the arduino uno are mounted on top of the servo motor, rotating along with the solar cell. This is where the problem begins: the servo motor is also connected to the arduino, and cannot rotate with itself.



The power supply and BTS7090 circuit, as well as the PID heating system additionally cannot be mounted on top of the servo to reduce the weight load on the servo. The connections between moving and nonmoving parts of the tracker mean that it is unable to track for more than 3 consecutive rotations in the same direction (>1080°). For most use cases, this is not an issue. For its intended purpose as a tracker for the sun, rotational range of motion greater than 1080° is not necessary. However, it is a flaw in the design that should be addressed in future iterations.

One way the tangled wiring issue can be addressed is by removing the LDRs entirely. Instead, a different approach to optimizing power output of the solar cell can be taken; instead of using a comparison of LDR values to move toward the point of maximum intensity, code can be written to maximize a voltage output reading using the solar cell itself as an input into the arduino. If LDR's are to be kept in the system, slip ring electrical connections could be used to ensure connections are maintained without tangling.

VI. Conclusion

This study successfully demonstrated the design, construction, and validation of an automated solar tracking system that significantly enhances photovoltaic energy harvest. Through systematic experimental investigation, we have quantified the fundamental relationships between solar cell performance and critical parameters like angle of incidence, implementing these relationships into tangible performance benefits in a solar tracking apparatus.

The experimental findings hold several significant implications for practical solar energy systems. First, the demonstrated 53.92% improvement in daily energy harvest indicates that tracking systems offer substantial benefits in applications of solar energy which produce power at a larger scale than the dissipated power of the tracking system itself.

The significant morning and evening performance advantages suggest that tracking systems effectively extend the productive generation period beyond traditional peak sunlight hours. This temporal distribution of power generation may align favorably with residential and commercial demand profiles, potentially reducing grid dependence during morning and evening peak usage periods when electricity costs are typically highest.

Several avenues for continued research and system optimization emerge from this work. The wiring entanglement issue represents the most critical mechanical design limitation requiring resolution. Implementing slip ring electrical connections or wireless power transmission could eliminate cable twisting while maintaining full rotational freedom. Alternatively, the proposed solar-cell-feedback approach could remove the need for separate LDR sensors entirely, simplifying mechanical design and potentially improving tracking accuracy by directly optimizing the parameter of interest. Expanding environmental characterization would strengthen



understanding of real-world performance variability. Systematic testing across different seasons, cloud conditions, and atmospheric clarity levels would help quantify how tracking advantages vary with environmental factors.

Advanced control algorithms incorporating solar position calculations could supplement or replace purely sensor-based tracking. Hybrid approaches combining algorithm-based positioning with sensor feedback for cloud-response could optimize performance more broadly, maintaining a high power output under partially cloudy conditions while reducing mechanical wear from continuous adjustment. Material selection optimization, particularly investigating anti-reflective coatings to minimize Fresnel losses at extreme angles, could further enhance performance [12].

This research successfully demonstrated that automated solar tracking substantially enhances photovoltaic energy harvest through maintaining optimal sun alignment throughout the daily solar trajectory. The integration of theoretical analysis, controlled laboratory experimentation, and real-world field validation provides comprehensive characterization of tracking system performance and underlying physical principles. While mechanical design limitations require attention in future iterations, the fundamental viability and significant performance advantages of automated solar tracking have been conclusively established. As global renewable energy deployment accelerates, optimization technologies such as solar tracking will play an increasingly important role in maximizing energy yield from photovoltaic installations.

VII. References

- [1] Gulomov, J., Aliev, R., Mirzaalimov, A., Mirzaalimov, N., Kakhkhorov, J., Rashidov, B., & Temirov, S. (2021). Studying the effect of light incidence angle on photoelectric parameters of solar cells by simulation. International Journal of Renewable Energy Development, 10(4), 731-736.
- [2] Ibrahim, N. I., & Baher Edin Omer, M. M. (2020, August). The effect of wavelength of light on solar electrical performance. In ASME Power Conference (Vol. 83747, p. V001T08A003). American Society of Mechanical Engineers.
- [3] Sun, C., Zou, Y., Qin, C., Zhang, B., & Wu, X. (2022). Temperature effect of photovoltaic cells: a review. Advanced Composites and Hybrid Materials, 5(4), 2675-2699.
- [4] Logan, P. E., & Raichle, B. W. (n.d.). PERFORMANCE COMPARISON OF FIXED, SINGLE, AND DUAL AXIS TRACKING SYSTEMS FOR SMALL PHOTOVOLTAIC SYSTEMS WITH MEASURED DIRECT BEAM FRACTION. https://ases.org/wp-content/uploads/2021/11/Performance-Comparison-of-Fixed-Single-a nd-Dual-Axis-Tracking-Systems-For-Small-Photovoltaic-Systems-with-Measured-Direct-B eam-Fraction-.pdf
- [5] Bolinger, M., Seel, J., Kemp, J. M., Warner, C., Katta, A., & Robson, D. (2023). Utility-Scale



- Solar, 2023 Edition: Empirical Trends in Deployment, Technology, Cost, Performance, PPA Pricing, and Value in the United States | Energy Markets & Policy. Lbl.gov. https://emp.lbl.gov/publications/utility-scale-solar-2023-edition
- [6] Bhuyain, M. T. M., Kuri, R., Bhuiyan, N. A., Sagor, M. S. H., & Haidar, R. (2021). Design and development of a single-axis solar tracking system. International Multidisciplinary Research Journal, 11, 13-24.
- [7] Muhsin, A. H., & Yousif, S. T. (2018). Horizontal single axis solar tracker using Arduino approach. Indonesian Journal of Electrical Engineering and Computer Science, 12(2), 489-496.
- [8] Shalwala, R. A. (2025). Using solar tracking technologies to enhance the efficiency of solar panels. Power Engineering Journal, 49(2), 2569-2581.
- [9] Algarni, S., Tirth, V., Alqahtani, T., Alshehery, S., & Kazi, S. (2022). Experimental investigation and comparison of the net energy yield using single- and dual-axis solar tracking systems. International Journal of Energy Research, 46(10), 14000-14018.
- [10] Schallenberger, B. B., Duminelli, E. C., de Araújo, J. C., & Urbanetz Junior, J. (2022). Study of the efficiency of the solar tracker system compared to the fixed system. Research, Society and Development, 11(5), e52811528493.
- [11] Lvovsky, A. I. (2013). Fresnel equations. Encyclopedia of Optical Engineering, 27, 1-6.
- [12] Shanmugam, N., Pugazhendhi, R., Madurai Elavarasan, R., Kasiviswanathan, P., & Das, N. (2020). Anti-reflective coating materials: A holistic review from PV perspective. Energies, 13(10), 2631.